Progresses on structure and functionality of vapor-deposited polymers as thin films and in multilayers

Anna Maria Coclite*

Institute of Solid State Physics, NAWI Graz, Graz University of Technology, Petersgasse 16, 8010 Graz, Austria

*Corresponding author: Tel: (+43) 316 873 8970; E-mail: anna.coclite@tugraz.at

Received: 08 November 2016, Revised: 29 November 2016 and Accepted: 13 December 2016

DOI: 10.5185/amlett.2017.1484
www.vbripress.com/aml

Abstract

Functional organic thin films (< 100 nm) are typical components of current devices in a variety of fields, including microelectronics, biotechnology and microfluidics. The need for miniaturization and structuration has boosted the development of advanced thin film growth techniques that can be easily implemented in the manufacturing steps of current device production. This review aims at presenting the latest progresses made in the field of chemical vapor deposition (CVD) methods of organic thin films. In CVD processes, the chemicals are delivered through the vapor-phase to the substrate, without the use of solvents, with the advantage of enlarging the applicability of polymer thin films to fields where the presence of solvent is detrimental. Among other methods, the initiated Chemical Vapor Deposition (iCVD) will be reviewed. High control over chemical composition, structure and film functionality has been largely demonstrated by iCVD. This technique allows coating virtually any substrate with conformal polymers at very low energy consumption. The specific chemical composition and the nanoengineered thickness control are desirable parameters for driving application-specific properties into the material. Further development of this field will certainly lead to progresses on the use of polymers in functional devices, as electrolytes, stimuli-responsive materials, encapsulants for drug-delivery and as membranes or barriers for permeation. Copyright © 2017 VBRI Press.

Keywords: Chemical vapor deposition, functional thin film, polymer coatings.

Introduction

The latest generation of functional devices features nanocomponents, hierarchical structures and multilayers. Such high level of complexity requires fine control on the fabrication process in order to achieve the desired functionality. In this scenario, Chemical Vapor Deposition (CVD) methods that give the possibility of synthesizing thin film with engineered surface properties, functionalities and topography are very appealing. The inclusion of polymers into functional devices is recently being explored due to the cheapness, lightweight and the broad choice of chemical moieties that this class of materials offers **[1]**. The possibility to apply CVD methods to polymer synthesis has numerous advantages: (i) easy processability into ultra-thin film form and multilayers; (ii) absence of solvents; (iii) conformality; (iv) chemical tunability and specificity; (v) high uniformity and scalability **[2]**.

Conventional processes used to form polymer thin films require the use of solvents. CVD is instead completely dry, the monomers and active species are not dissolved in a common media but delivered through the vapor phase **[3]**. The absence of the dissolution-need favors the use of polymers in every-day applications where the presence of solvent entrained in the polymers would cause properties degradation and device failure. Biotechnology, for example, requires polymer thin films to be well adherent, chemically inert, free of leachable, plasticizer and insoluble **[4**, **5]**. Successful example of CVD polymers, which are stable over extended periods of time and resistant to solvent treatments, multiple exposures to heat, humidity and mechanical wear have been demonstrated and will be reviewed in the next sections **[6**, **7]**. The absence of solvent allows also combining monomers with completely different solubilities and obtaining unconventional copolymers without unwanted phase separation **[8]**.

CVD polymerizations have as common ground that they work in a mild-vacuum environment, and are governed by the adsorption of the polymer building blocks on the substrate, which is kept near room temperature. The retention of the monomer functional groups in the final polymer drives the desired refraction index **[9]**, surface energy **[10]**, conductivity **[11]**, etc. Some innovative CVD polymerization routes (e.g. initiated CVD, iCVD **[12]**, and initiated plasma enhanced CVD, iPECVD **[13]**) have demonstrated full retention of the monomers chemical structure at high growth rates (up to 500 nm/min), while this was possible by other CVD methods only by sacrificing the polymer growth rate (e.g. with pulsed plasma enhanced chemical deposition, pulsed-PECVD **[14]**).

The low operating temperature allows to deposit polymers on virtually any substrate, including unconventional delicate and flexible ones, such as paper or plastic, or on substrates, like hydrogels, which would swell upon solvent exposure **[15]**. Multilayer structures can also be easily deposited entirely by CVD just changing the deposition conditions from one layer to the other without the risk of dissolving the underlayer **[16]**.

Engineered three-dimensional shapes in terms of cavities or channels, for example, are important for device performance. Sensors, for example, highly benefit from large surface areas **[8]**. CVD polymers can uniquely provide additional properties by adding a thin film, assuming that the latter preserves the topography at the micro and nano-scale. Conformality is achieved when the thin film coats every contour of a geometric feature with uniform thickness **[17]**. CVD polymers can achieve high level of conformality by controlling the sticking and diffusion coefficients of the molecules on the surface.

In the next sections, the fundamentals of some CVD methods to deposit polymers will be reviewed with particular emphasis on the different structures that can be obtained, e.g. crystalline, cross-linked, and how these affects and drive the functionality of the specific polymer material. The focus will be on only the most recent application of CVD polymers, since the previous have been already reviewed in the past **[18]**.

Fundamentals on CVD of polymers

Similarly, to the classical solution polymerizations, the mechanism of CVD is based on three main steps: initiation or activation, chain polymer propagation and termination. The CVD polymerizations differ mainly for the first step. The activation can be thermal, photo-induced or plasma assisted **[19]**.

If there is plasma involved, like in PECVD polymerizations, the electronic collisions, typical of the plasma phase, fragment and/or ionize all gases that feed the plasma (a scheme for this is presented in **Fig. 1a**). The fragments then can react homogeneously in the plasma phase and when they have reached a certain size they adsorb on the substrate and react heterogeneously with the other adsorbed fragments or with the dangling bonds of the substrate. The mechanism of such polymerization is detailed in references **[20]**.

On the substrate, the polymer grows by addition of several fragments. Every surface exposed to the plasma has a negative potential, therefore it is subject to the positive ion bombardment. This creates more active sites on the substrate but also on the growing polymer, leading to further possible reaction pathways. The large number of reaction pathways that a monomer species can undergo during the plasma polymerization process makes it difficult to predict the final structure that the polymer will have. Since the electronic collisions are non-selective they can involve also the monomer vapors, inducing the loss of some labile functional groups. Different studies in literature, for example, report on how difficult it is to retain –COOH or $–NH_2$ groups in plasma polymers. **[21, 22]** To limit the damages to the monomer structures, “soft” conditions can be used: e.g. high pressure, low and often pulsed plasma power, resulting, as a drawback, in low deposition rates.

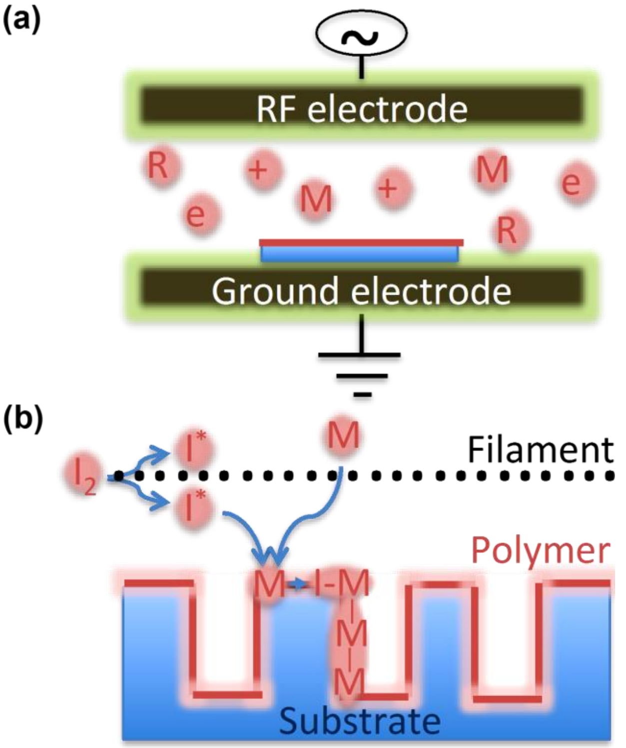

Fig. 1. Schematics of two CVD polymerization processes: (a) plasma polymerization (PECVD) (b) initiated CVD (iCVD).

On the other hand, organic polymers offer a great portfolio of physical properties (e.g. wettability, conductivity) depending on the chemical groups pending from the polymer chains. It is strategically important to plan which monomer units to chain together in order to carefully design the polymer chemistry. There are vapor-based polymerization methods, in which the activation step does not involve the fragmentation of the monomer. Examples of this latter type of polymerizations are iCVD **[23]**, iPECVD **[13]** and oxidative CVD (oCVD) **[24]**. In these processes, the monomers do not undergo any fragmentation but selective chemical reactions. In the iCVD, schematized in **Fig. 1b**, an initiator species is used as sacrificial molecule. This is thermally decomposed by a heated filament to create radicals that selectively react with the vinyl bonds of the monomer. The monomer units are not thermally decomposed because the filament is heated only to temperature > 300- cvccb°C, which is high enough to break the labile bonds of the initiator but not high enough to decompose the monomer. Therefore, the monomer units arrive intact to the substrate where they get adsorbed. The initiator radicals hitting with the substrate surface zip together the monomer units as in a conventional radical polymerization. The total absence of ion bombarding favors the growth of polymer with fewer defects compared to plasma polymers. This can lead to enhanced photo-stability and slower material aging **[25]**.

A similar mechanism governs the most recently developed iPECVD technique **[26, 27]**. In this case the initiator radicals are created by a very weak plasma discharge. The very low plasma power is able to fragment almost exclusively the initiator, retaining the whole monomer structure **[13]**. High powers instead would fragment also the monomer together with the initiator, resulting again in the loss of the monomer structure retention.

Together with retaining the monomer chemical functionalities, iCVD, iPECVD and oCVD coatings can conformally cover complex geometrical features. Polymers that are obtained from conventional solution synthesis often show meniscus formation or de-wetting, liquid thinning and other solvent surface tension effects, which alter the profile of the coating on the substrate. Much better conformality is obtained from the vapor-phase when the sticking probability of the reactants to the surface during a single collision is kept low. Sticking coefficients in the range of ca. 0.001–0.01 have been observed for iCVD. The ratio between monomer partial pressure (P_M) and the pressure at which the monomer vapors condense and saturate on the surface (P_{sat}) can be used as governing parameter to drive iCVD from conformal (at low P_M/P_{sat}) to unconformal (at P_M/P_{sat} close to 1). The latter condition can be used, for example to coat porous substrates with the aim of filling the pores **[28]**.

Structure of CVD polymers

Crystalline polymers

The CVD polymers most commonly aggregate in amorphous states. Nevertheless, a few examples exist in literature of CVD polymers that actually show crystalline aggregation. This was mostly observed for fluorinated polymers, where the $-CF_2-$ units tend to pack together to minimize the surface energy **[29]**. Semicrystalline chains of poly-tetrafluoroethylene-like (PTFE) polymers were obtained by Milella et al. via pulsed-PECVD **[30]**. They observed ribbon-like features on the samples that showed high crystallinity. The PTFE is a linear polymer made of CF_2 repeating units that naturally aggregates in helical smectic B lamellae **[31]**. The PTFE-like obtained by PECVD, though, had also a high fraction of CF and CF_3 groups, generated by the monomer fragmentation discussed in the previous section. The crystallinity in this case was related with the monomer structure retention and it was observed only for the samples deposited in pulsed conditions where the CF_2 ratio in the polymer was the highest.

Another example of crystalline CVD polymer was the poly-(1H, 1H, 2H, 2H -perfluorodecylacrylate) (p-PFDA) obtained by iCVD **[32]**. Such polymer contains an eight-units-long pendant chain that form aggregates in an ordered lamellar structure called smectic B phase with a periodicity of 32.4 Å as shown in **Fig. 2a**.

The characteristic of the iCVD process to retain the monomer chemical structure allowed obtaining linear PFDA polymers with long fluorinated pendant chain that formed a succession of bilayers of pendant perfluorinated groups coming alternatively from two different polymer chains. These polymers showed also a preferential orientation, with the axes of the side perfluorinated chains perpendicular to the plane of the hexagonal lamellar packing and a lattice parameter of 6.4 Å. Depending on the deposition conditions and in particular the initiator over monomer ratio (I/M, as indicated in **Fig. 2b**) it was possible to obtain different degrees of crystallinity. Sharp intense Bragg peaks were obtained at I/M value of 4. Those were strongly dampened at higher I/M values.

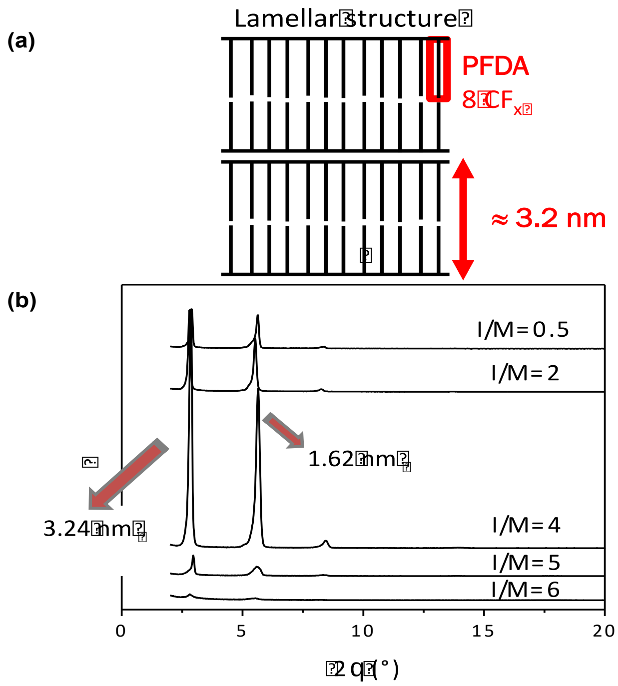

Fig. 2. (a) Lamellar structure of the poly-perfluorodecylacrylate (p-PFDA) deposited by iCVD. (b) X-ray diffractograms are shown for films deposited at different initiator over monomer (I/M) ratios. Adapted with permission from ref. **[32].** Copyright 2012 WILEY-VCH.

The packing of the side can drive important materials properties, such as remanent polarization, piezoelectricity, and elasticity. Also the wetting properties of polymers containing fluorinated side chains can be markedly influenced by the packing of the side chains resulting from crystallization **[10]**. In the section 3.1, the link between crystalline structure and polymer functionality will be demonstrated for proton conductivity on a copolymer of PFDA.

Cross-linked polymers

Another advantage of depositing from the vapor phase is that cross-linked polymers can be easily obtained in a thin film form, regardless of their insolubility, which instead severely limits the spin coating or casting processes. A certain degree of cross-linking is desirable for applications where mechanical stability is also required **[33].** Coatings for biological implantations are an example of this category: the coating in this case needs to be adherent to the prosthesis and do not leak or delaminate in the body. Plasma polymers are naturally cross-linked since the polymer is always exposed to a certain extent of ion bombarding, which creates dangling bonds and cross-links **[34]**. It also naturally covalently binds the polymer to the substrate, improving the adhesion and avoiding issues related to delamination. Ion bombarding is totally absent in the iCVD process; therefore, in this case separate chemical species have to be added both to cross-link the polymer and to improve its adhesion to the substrate **[24]**. Cross-linking species for iCVD are molecules with two or more vinyl bonds (e.g. ethylenglycoldimethacrylate, EGDMA). The addition of a separate chemical cross-linker has the advantage that a certain control over the cross-linking degree can be attainable by iCVD. The ratio monomer over cross-linker flow rate in the gas feed can be adjusted and optimized to obtain the desired mesh size **[35]**. The mesh size is the distance between two consecutive cross-links. Antifouling coatings can be obtained by smartly targeting a determined mesh size that is smaller than the foulants.

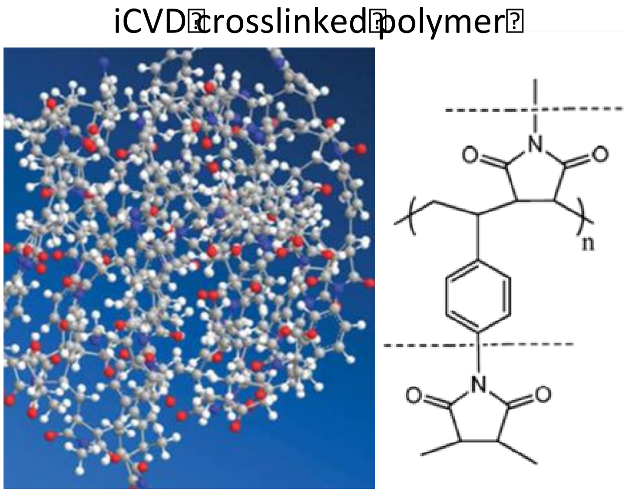

Fig. 3. 3-D and 2-D molecular structure of annealed poly (4-aminostyrene-alt-maleic anhydride). The structures were obtained from Chem3D software, by running a molecular dynamics simulation. Reproduced with permission from ref. **[7].** Copyright © 2012 WILEY-VCH Verlag GmbH & Co. KGaA, Weinheim.

Highly cross-linked but yet flexible coatings have also been obtained by iCVD, by controlling the mean connectivity number (<r>) **[7]**. This is the average number of possible network forming bonds per atom: **[36]**.

$$\langle r\rangle = \frac{\sum_r r n_r}{\sum_r n_r}$$

with n_r being the number atoms having r network forming bonds. Amorphous films are characterized by connectivity numbers between 2 and 3. If the connectivity number of the network is low, i.e. between 2 and 2.4, the polymer is underconstrained and flexible. Higher number of cross-links can lead to an overconstrained and rigid network. The cross-linked network showed in **Fig. 3** corresponds to the annealed copolymer of 4-aminostyrene and maleic anhydride. After annealing intra chain covalent amidic bonds form, which cross-link the polymer and increase its connectivity number from 2.308 in the as-deposited polymer to 2.385 after annealing. Both values are below 2.4 and indeed the polymer survived repeated folding test (to 200 times) without showing cracking or delamination. The oxygen permeability observed for the annealed coating was also lower than those of commercial polymers.

High cross-linking was also demonstrated on organosilicon polymers, obtained from the polymerization of hexavinyldisiloxane. The presence of six vinyl bonds in the monomer unit induces high levels of crosslinking. Nevertheless, some vinyl bond remained unreacted, resulting in a connectivity number of 2.1, typical of cross-linked yet flexible polymers.

From structure to functionality

Polyelectrolytes

Polyelectrolytes are polymers containing groups that dissociate in aqueous solutions, creating charges on the polymer chains. Typical examples are poly-acrylic acid, poly-vinylimidazole, poly-aminostyrene.

Proton exchange membranes (PEM) are made of polyelectrolytes. They allow the selective passage of protons or more in general cations. Typically, PEMs are made of a perfluorinated matrix on which proton-exchange groups such as phosphonic acid ($–PO_3H$), carboxylic acid (–COOH), or more often, sulfonic acid ($–SO_3H$) are grafted. In water solution, the acid groups get deprotonized, so they assume a negative charge that allows the passage of H^+, through the membrane. The perfluorinated matrix serves the purpose of ensuring integrity to the polymer backbone when immersed in water. The proton transport in hydrated PEMs is speculated to occur through "ionic channels" which are interconnected hydrophilic clusters embedded inside the hydrophobic matrix **[37]**.

Copolymers made of hydrophobic and hydrophilic monomers were deposited by iCVD starting from perfluorodecylacrylate (PFDA) and methacrylic acid (MAA) as monomers **[38]**. Spectroscopic evidences showed that iCVD allowed to obtain copolymer with both acid and fluorinated functionalities retention. Copolymers with different composition were deposited by simply changing the monomer fraction in the gas feed. The copolymerization was demonstrated to follow a moderate alternated behavior of MAA and PFDA units, with calculated reactivity ratio <1, meaning that when a MAA unit is terminating the polymer chain, it preferably reacts with a PFDA unit and vice versa. The reactivity ratios describe the propensity of the propagating species to add a homomonomer or the other monomer. The surface elemental composition of the copolymer exhibited dynamic changes before and after soaking in water: in the dry state the surfaces were enriched of fluorinated groups while in the hydrated state the ratio F/C decreased. In air, the hydrophobic fluorinated chains preferably orient outward at the surface while the hydrophilic carboxylic pendant group of MAA orient inward in order to minimize the surface energy.

A follow-up study demonstrated that the copolymers crystallize into a bilayer lamellar structure, formed by the perfluorinated pendant chains of PFDA, while the MAA units orient outside the lamellae **[39]**. Similarly, to the structure depicted in **Fig. 2**, the perfluorinated chains orient perpendicularly to the substrate surface. Among the bilayers, the MAA molecules form COOH-enriched regions, which can act as ionic channels for proton conduction when the acid groups are deprotonated into COO^-. This structure is schematized in **Fig. 4a**.

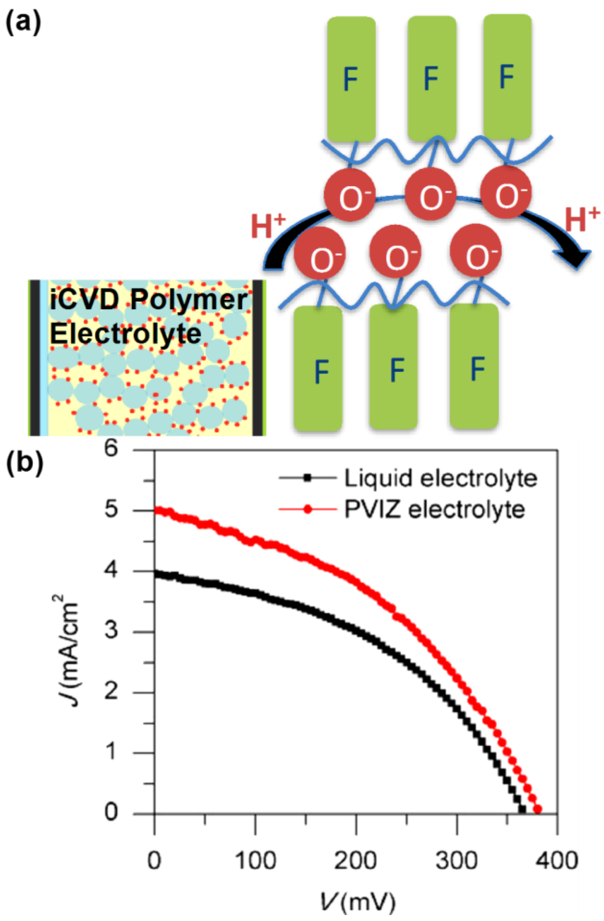

Fig. 4. (a) Schematic of the layered structure observed for the MAA-PFDA copolymer deposited by iCVD. The rectangles labeled with “F” indicate the perfluorinated chains, while the circles labeled with O^- indicate the deprotonated –COOH groups. (b) Current-voltage characteristics of a dye-sensitized solar cell containing a polymer electrolyte (PVIZ) and another one with a liquid electrolyte. (b) Reproduced with permission from ref. **[40]** Copyrights 2016 Elsevier.

Other examples of polyelectrolytes are polymers bearing electronegative rings, like polysiloxanes and polysilazanes, to which small cations can bind. **[41]** Those have shown ionic conductivity at the nanoscale.

Polyelectrolytes are also used in dye-sensitized solar cells. Typically, the electrolytes used in these solar cells are liquid; limiting the performance of the devices with leakage, metal contact corrosion and evaporation issues. It has been demonstrated that polymer electrolytes deposited from iCVD lead to higher performance and allow to tune the current-voltage (J–V) behavior of the cell **[42]**. Two types of dye-sensitized solar cells are compared in **Fig. 4b**. In one case, the photoanode is coated with a cross-linked poly-vinylimidazole (PVIZ) electrolyte by iCVD, and exposed to the acetonitrile liquid electrolyte containing an iodide/triiodide redox couple to incorporate the redox couple in the PVIZ **[40]**. In the other case, the cell contains the uncoated photocathode and the liquid electrolyte with the redox couple. It is evident form **Fig. 4** that having the redox couple incorporated into the PVIZ improves the current-voltage characteristic of the dye-sensitized solar cell, when compared to the case in which the redox couple was dissolved into the liquid electrolyte. The suggested reason for the higher current density obtained with the PVIZ was related to the basic nature of the imidazole group, which can then give acid-base interactions with the TiO_2 electrode and form a strong blocking layer to reduce the electron recombination rate.

Stimuli responsive polymers

Stimuli-responsive materials are characterized by dynamic switching of their properties depending on external stimuli (e.g. exposure to some gases, changes in temperature or pH). Responsive elements may be anisotropic deformation, non-linear stress-strain behavior and electrical, thermal and/or optical changes to the elastic modulus of the material framework. Nature is full of examples of responsive materials, such as the skin of lizard or cuttlefish, which change their body patterns and colors depending on the surrounding environment. Recently, numerous synthetic examples of responsive surfaces have emerged, which rely on conformational changes in the polymer network, or pattern modifications **[43]**.

Hydrogels are known for their dynamic swelling response to aqueous environments. The hydrogel swelling in water results in changes in the mechanical properties, protein adsorption capabilities and hydrophilicity of the polymer **[44, 45]**. PHEMA (poly-2, hydroxyethyl methacrylate) is one of the most studied hydrogel. Fast and reversible changes in the thickness of hydrogels were used in impedance sensors to control the passage of the analyte or for controlled drug delivery systems **[46, 47]**.

The stimuli-responsiveness is linked with the number of functional groups that can be preserved during the vapor-based polymerization. Highly responsive (to water and water vapors) pHEMA hydrogels have been deposited by iCVD process **[48, 49]**.

Thermo-responsive polymers are known for their dynamic swelling in response to temperature in aqueous environments. The temperature induces a change from coil-to-globule in correspondence of the lower critical solution temperature (LCST). The most investigated thermoresponsive polymer is the poly-N-isopropylacrylamide (pNIPAAm), whose LCST can vary between 14 and 40 °C depending on the copolymer hydrophobicity, and on the ability to form H-bonding with the adsorbed water **[50]**. In addition, the LCST can be varied with the number of carbon atoms on the alkyl group or the number of alkyl groups bonded to the amide group. Fast response is achieved in the temperature range LCST ± 4 °C **[51]**.

Resistive sensors can also be based on stimuli-responsive materials. Carbon nanotubes, for example, in presence of volatile organic compounds (VOCs) change their electrical resistance. Recently a hybrid material made of vertically aligned carbon nanotubes (VA-CNTs) and poly-3,4-ethylenedioxythiophene (PEDOT) showed large sensitivity to n-pentane **[52]**. Being the latter, non-polar, this is an important addition to the library of VOCs detectable by carbon nanotubes. The PEDOT behave also as responsive material, indeed in presence of the analyte the electron-hopping rate decreases, increasing the resistance **[8]**. The PEDOT was deposited by oCVD and it conformally coated the VA-CNT forest. **Fig. 5** shows how the fast and reversible resistive response of the hybrid system to even very small quantity of n-pentane.

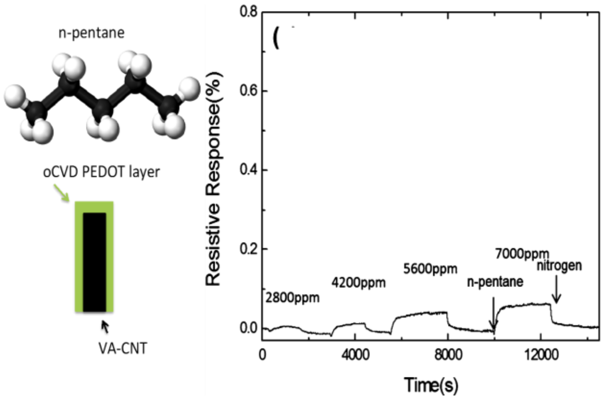

Fig. 5. Resistive response to vapors of n-pentane of hybrid nanotubes made of carbon and conformally coated with PEDOT. Reproduced with permission from **[52]**. Copyright 2016 American Chemical Society.

Polymers for controlled drug delivery

The engineering of the surface chemistry and properties has allowed the successful integration of CVD polymers into prototypes for applications including controlled drug release **[53**]. The CVD polymer acts as a shell, protecting the drug and allowing a site-specific delivery. The controlled vacuum environment and the high purity of commercially available monomeric reactants enable a highly reproducible layer production, a must for safe medical application. The encapsulation process must be gentle to avoid drug degradation and the end products free of plasticisers and leachable. In this scenario, CVD processes that run at low temperatures and in a dry environment can offer interesting solutions.

Enteric release can, for example, be obtained with pH-responsive encapsulants. At low pH, i.e. in the stomach, the meshes of the polymer are in a collapsed globule shape, so the drug cannot be released. At high pH, i.e. in the lower part of the intestine, the polymer meshes swell, allowing the timed delivery of the drug and avoiding deteriorating the drug efficiency during the transit to the specific target. Copolymers of methacrylic acid (MAA) deposited by iCVD have been demonstrated for enteric release **[54]**. The copolymers were also deposited directly on fine ibuprofen microcrystals. The release of uncoated and coated ibuprofen at pH 7.4 was relatively fast in both cases. On the contrary, at pH 1.2, the release through the encapsulation was significantly delayed. The same copolymer was also deposited on biodegradable porous Si support, loaded with the drug **[46**, **55]**.

In **Fig. 6** an example of polymer encapsulation made by iCVD is shown **[56**, **57]**. The encapsulated drug was clotrimazole. This was deposited as a thin molecular layer on a substrate. The bare drug crystallised within 48h at room temperature, as evident from the crystalline islands showed in the top left micrograph. Crystalline drug layers show a poor solubility and low bioavailability; therefore it is important to find new strategies and conditions that allow to keep the drug into the amorphous state **[58]**. By engineering the iCVD layer, a prolongation of the clotrimazole amorphous state was achieved. The top right and bottom micrographs of **Fig. 6** show the surface of three different polymer encapsulants after 48h storage at room temperature. In all three cases, the number of crystallites (which appear as bright areas in the images) is considerably less compared to the bare drug.

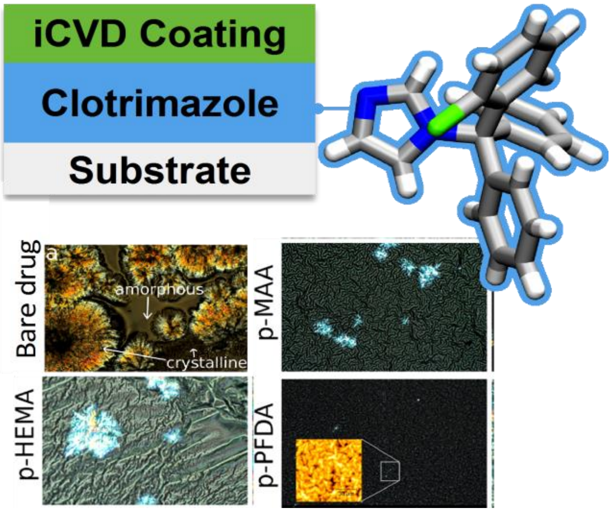

Fig. 6. (Top) Schematics of the clotrimazole encapsulation. (Bottom) Optical micrographs of the surface of the bare drug and of the drug encapsulated with three different polymers deposited by iCVD. Adapted with permission from **[57].**

Other examples of controlled releases were achieved on nanotubes. Those have large surface area; therefore they can be loaded with and release large quantity of macromolecules. In addition to this, their surface can be modified by applying a conformal coating. Using coatings that are responsive allows to switch, then, the release externally. Burst release was obtained for example by coaxial nanotubes of a shape memory polymer and a hydrogel core, at elevated temperature **[59]**. Tunable release was also observed with responsive hydrogels **[60]**. The release studies from nanotubes were both demonstrated on dyes as models, but the same technology can be easily applied to delivery of actual drugs.

Polymer-based composites and multilayers for selective diffusion

Many interesting fields of applications are based on selective diffusion, e.g. membrane technology, packaging, microfluidics. Conformal coatings on pores can enhance the selectivity of a membrane towards specific gases, vapors or liquids, for example, or alternating polymers with inorganic layers can enhance the barrier properties towards gas and vapors.

Currently, one of the difficulty that is limiting the wide spread commercialization of flexible electronic devices is their sensitivity to oxygen and water vapors, which can permeate easily through non-rigid substrates. Hence, considerable research effort is devoted to the development of barrier thin films that can be deposited on the flexible-substrates, without affecting the lightweight and the mechanical properties of the latter, but considerably limiting the diffusion through them. The most promising strategy consists in the use of multilstacks in which inorganic glass-like layers are alternated with polymers. The polymer layers have the role of smoothening and filling the pores of the substrate and of the other inorganic layer and offer a microscopically flat surface for the deposition of the subsequent inorganic layer **[61]**. Promising performances have been obtained by polymers deposited by iCVD **[9**, **62]** and iPECVD **[63]**. Both inorganic (SiO_x, SiN_x) and polymer (acrylate, silicone) layers can be easily deposited by CVD methods in single-chamber deposition processes by coupling PECVD and iCVD **[16]**, or hot wire CVD with iCVD **[64-66]**.

Selective permeation is the ground principle of membrane technology. Membranes are engineered to allow the passage of solutions and block some components contained in the solution. Common examples are desalination membranes. iCVD coatings have been used to enhance selective permeation of commercially available membranes or as membranes themselves. In order to achieve membrane distillation for desalination, the membrane must show high permeability to water vapors, but high liquid entry pressure, so the saline water cannot permeate. The liquid entry pressure is enhanced when commercial membranes are coated with hydrophobic layers. The coating in this case must be ultra-thin and conformal in order not to reduce too much the average pore size **[67]**. Another example in which the iCVD coating enhanced the selective permeation of commercial membrane was demonstrated by Kim *et al.* **[68]**. They coated a sponge with a hydrophobic coating. The combination of porosity and fluorinated chemistry made the surface of the sponge superhydrophobic and superoleophobic, therefore ideal for a gas-permeable liquid separator.

Unconformal coatings can also be used for thin film composite membranes, depending on which type of separation process they are devoted to. Facilitated transport of Cr(VI) was obtained by a continuous defect-free "blanket-type" coating deposited by iCVD over a porous fabric support **[69]**. Surface modification can also be used to prevent membrane fouling. A copolymer of HEMA and PFDA was deposited on reverse osmosis membranes using iCVD and exhibited superior antifouling performance compared to the bare membrane **[70]**.

Outstanding gas-separation performances for multiple gas pairs was achieved by metal-organic covalent networks obtained by iPECVD **[71**, **72]**. The presence of the metal Zn coordinated with the porphyrin rings allowed for the separation of CO_2/CH_4, H_2/N_2 and H_2/CH_4. Alternatively, the iCVD polymer can be the membrane itself, since it can have engineered porosity **[73]** or mesh size. Size exclusion permeation was obtained by fine-tuning of the pHEMA mesh size in freestanding polymers **[74]**. Asymmetric polymer membranes were deposited by continuously changing the deposition conditions from the ones resulting in a dense layer to the ones yielding into a porous polymer **[75]**. In addition to the asymmetric structure, also the chemical functionality of the two layers could be independently chosen. This approach can be applied to the separation of small molecules based on chemical affinity for various applications such as pharmaceutical purification, kidney dialysis, and water desalination.

Conclusion and future perspectives

CVD polymers can have designed properties, which lead to interesting functionalities and enable multiple technological applications. This review summarizes the latest results in terms of controlling the film properties (e.g. cristallinity and cross-linking) and functionalities. The fine engineering of the film properties allows obtaining the desired functionalities, which makes of the CVD thin film desirable components of current devices. CVD polymers have been demonstrated to serve as polyelectrolytes for solar or fuel cells, as stimuli-responsive materials as required for sensor, as encapsulants for targeted drug delivery, and to enable selective diffusion through membranes.

The field is not limited to what has been presented; indeed CVD polymers have been successfully implemented into functional devices and industrial processes. Recent examples are organic thin film transistors, in which the gate insulator was a polymer deposited by iCVD **[76]**, organic complementary inverters in which the iCVD polymer acted as dielectric layer **[77]** and polymer-based memory arrays whose active component was again obtained by iCVD**[78]**. The properties that allowed such implementation were the possibility to deposit ultra-thin coatings with tunable profiles from conformal to unconformal and the possibility to coat also delicate substrates, which would instead be damaged by other types of processes. The range of applications for CVD polymers is rapidly growing and it is anticipated to expand into new fields like robotics and biomedicine. A wide range of homopolymers and copolymer compositions have been demonstrated by iCVD, iPECVD and oCVD. All these methods are characterized by high monomer structure retention, so the chemical functionalities can be retained in the thin film polymer. This allows translating the large variety of polymers obtainable by conventional organic synthesis into thin films that can be ultra-thin, uniform over large area and conformal. Unconventional chemistries can also be obtained since the monomers used for the copolymerization do not require a common solvent. Large-scale, roll-to-roll deposition chambers are used for practical industrial applications. Reproducible processing from lab to industrial scale was obtained by scaling up vapor flow patterns during the delivery of reactants, and reaction temperatures. Deeper knowledge on the process will further boost the clustering of polymer deposition techniques with the classical inorganic deposition methods, to achieve fully automated deposition routines for hybrid systems.

Acknowledgements

The author acknowledges financial support from Marie Curie International Incoming Fellowship within the 7th European Community Framework Programme.

References

1. Moon, H.; Seong, H.; Shin, W. C.; Park, W. T.; Kim, M.; Lee, S.; Bong, J. H.; Noh, Y. Y.; Cho, B. J.; Yoo, S.; Im, S. G., *Nat Mater* **2015,** *14* (6), 628. **DOI:** 10.1038/nmat4237.
2. Gleason, K. K. (Eds.), *CVD Polymers: Fabrication of Organic Surfaces and Devices*, Wiley -VCH Verlag GmbH & Co. KGaA: Weinheim, Germany, **2015**. **DOI:** 10.1002/9783527690275.
3. Ozaydin-Ince, G.; Coclite, A. M.; Gleason, K. K., *Rep. Prog. Phys.* **2012,** *75* (1), 1. **DOI:** 10.1088/0034-4885/75/1/016501.
4. Coclite, A. M., CVD Polymer Surfaces for Biotechnology and Biomedicine. In *CVD Polymers: Fabrication of Organic Surfaces and Devices*, Gleason, K. K., Ed. Wiley-VCH Verlag GmbH & Co. KGaA, Weinheim, Germany: **2015**. **DOI:** 10.1002/9783527690275.ch14.
5. De Luna, M. M.; Chen, B.; Bradley, L. C.; Bhandia, R.; Gupta, M., *J. Vac. Sci. & Technol. A* **2016,** *34* (4). **DOI:** 10.1116/1.4953876.
6. Bakker, R.; Verlaan, V.; van der Werf, C. H. M.; Rath, J. K.; Gleasonb, K. K.; Schropp, R. E. I., *Surf. & Coat. Technol.* **2007,** *201* (22-23), 9422. **DOI:** 10.1016/J.Surfcoat.2007.03.058.
7. Xu, J.; Asatekin, A.; Gleason, K. K., *Adv. Mat.* **2012,** *24* (27), 3692, **DOI:** 10.1002/adma.201201197
8. Bhattacharyya, D.; Senecal, K.; Marek, P.; Senecal, A.; Gleason, K. K., *Adv Func. Mat.* **2011,** *21*, 4328. **DOI:** 10.1002/adfm.201101071.
9. Aresta, G.; Palmans, J.; van de Sanden, M. C. M.; Creatore, M., *J. Vac. Sci. & Technol. A* **2012,** *30* (4). **DOI:** 10.1116/1.4711762
10. Coclite, A. M.; Shi, Y.; Gleason, K. K., *Adv Mater* **2012,** *24* (33), 4534. **DOI:** 10.1002/adma.201200682.
11. Barr, M. C.; Carbonera, C.; Po, R.; Bulovic, V.; Gleason, K. K., *Appl. Phys. Lett.* **2012,** *100* (18). **DOI:** 10.1063/1.4709481.
12. Coclite, A. M.; Howden, R. M.; Borrelli, D. C.; Petruczok, C. D.; Yang, R.; Yague, J. L.; Ugur, A.; Chen, N.; Lee, S.; Jo, W. J.; Liu, A.; Wang, X.; Gleason, K. K., *Adv Mater* **2013,** *25* (38), 5392. **DOI:** 10.1002/adma.201301878.
13. Coclite, A. M.; Gleason, K. K., *Plasma Proc. Polym.* **2012,** *9* (4), 425. **DOI:** 10.1002/Ppap.201100167.
14. Tamirisa, P. A.; Liddell, K. C.; Pedrow, P. D.; Osman, M. A., *J. Appl. Polym. Sci.* **2004,** *93* (3), 1317. **DOI:** 10.1002/app.20498.
15. Barr, M. C.; Rowehl, J. A.; Lunt, R. R.; Xu, J.; Wang, A.; Boyce, C. M.; Im, S. G.; Bulovic, V.; Gleason, K. K., *Adv Mater* **2011,** *23* (31), 3499. **DOI:** 10.1002/adma.201101263.
16. Coclite, A. M.; Ozaydin-Ince, G.; Palumbo, F.; Milella, A.; Gleason, K. K., *Plasma Proc. Polym.* **2010,** *7* (7), 561. **DOI:** 10.1002/ppap.200900139.
17. Baxamusa, S. H.; Gleason, K.K., *Chem. Vap. Dep.* **2008,** *14* (9-10), 313. **DOI:** 10.1002/cvde.200806713.
18. Yagüe, J. L.; Coclite, A. M.; Petruczok, C.; Gleason, K. K., *Macromol. Chem. Phys.* **2013,** *214* (3), 302. **DOI:** 10.1002/macp.201200600.
19. Burkey, D. D., Non-Thermal Initiation Strategies and Grafting. In *CVD Polymers: Fabrication of Organic Surfaces and Devices*, K.K.Gleason, Ed. Wiley-VCH Verlag GmbH & Co. KGaA: Weinheim, **2015**. **DOI:** 10.1002/9783527690275.ch4.
20. Yasuda, H.; Hirotsu, T., *J. Polym. Sci.: Polym. Chem. Ed.* **1978,** *16* (4), 743. **DOI:** 10.1002/pol.1978.170160403.
21. Sherazi, T. A.; Guiver, M. D.; Kingston, D.; Ahmad, S.; Kashmiri, M. A.; Xue, X., *J. Power Sources* **2010,** *195* (1), 21. **DOI:** 10.1016/j.jpowsour.2009.07.021.
22. Urstöger, G.; Resel, R.; Koller, G.; Coclite, A. M., *J. Appl. Phys.* **2016,** *119* (13), 135307. **DOI:** 10.1063/1.4945578.
23. Coclite, A. M., *Surf. Innovations* **2013,** *1* (1), 6. **DOI:** 10.1680/si.12.00019.
24. Im, S. G.; Gleason, K. K., *AIChE J.* **2011,** *57* (2), 276. **DOI:** 10.1002/aic.12522.
25. Baxamusa, S. H.; Suresh, A.; Ehrmann, P.; Laurence, T.; Hanania, J.; Hayes, J.; Harley, S.; Burkey, D. D., *Chem. Vap. Dep.* **2015,** *21* (10-12), 267. **DOI:** 10.1002/cvde.201507173.
26. Hilt, F.; Boscher, N. D.; Duday, D.; Desbenoit, N.; Levalois-Grutzmacher, J.; Choquet, P., *ACS Appl Mater Interfaces* **2014,** *6* (21), 18418. **DOI:** 10.1021/am504892q.
27. Gürsoy, M.; Karaman, M., *Phys. Status Solidi C* **2015,** *12* (7), 1006, **DOI:** 10.1002/pssc.201510034.
28. Hsieh, C.-Y.; Lau, K. K. S., *Adv. Mater. Interfaces* **2015,** *2* (17), 1500341. **DOI:** 10.1002/admi.201500341.
29. Honda, K.; Morita, M.; Otsuka, H.; Takahara, A., *Macromolecules* **2005,** *38* (13), 5699. **DOI:** 10.1021/ma050394k.
30. Milella, A.; Di Mundo, R.; Palumbo, F.; Favia, P.; Fracassi, F.; d'Agostino, R., *Plasma Proc. Polym.* **2009,** *6* (6-7), 460. **DOI:** 10.1002/ppap.200930011.
31. Brown, E. N.; Rae, P. J.; Dattelbaum, D. M.; Clausen, B.; Brown, D. W., *Exp. Mech.* **2007,** *48* (1), 119. **DOI:** 10.1007/s11340-007-9075-3.
32. Coclite, A. M.; Shi, Y. J.; Gleason, K. K., *Adv. Funct. Mat.* **2012,** *22* (10), 2167. **DOI:** 10.1002/Adfm.201103035.
33. Bose, R. K.; Lau, K. K. S., *Biomacromolecules* **2010,** *11* (8), 2116. **DOI:** 10.1021/bm100498a.
34. Karaman, M.; Uçar, T., *Appl. Surf. Science* **2016,** *362*, 210. **DOI:** 10.1016/j.apsusc.2015.11.254.
35. Yagüe, J. L.; Gleason, K. K., *Soft Matter* **2012,** *8* (10), 2890. **DOI:** 10.1039/C2sm07137a.
36. He, H.; Thorpe, M. F., *Phys Rev Lett* **1985,** *54* (19), 2107. **DOI:** 10.1103/PhysRevLett.54.2107.
37. Schmidt-Rohr, K.; Chen, Q., *Nat Mater* **2008,** *7* (1), 75. **DOI:** 10.1038/nmat2074.
38. Coclite, A. M.; Lund, P.; Di Mundo, R.; Palumbo, F., *Polymer* **2013,** *54* (1), 24. **DOI:** 10.1016/j.polymer.2012.11.004.
39. Ranacher, C.; Resel, R.; Moni, P.; Cermenek, B.; Hacker, V.; Coclite, A. M., *Macromolecules* **2015,** *48* (17), 6177. **DOI:** 10.1021/acs.macromol.5b01145.
40. Kuba, A. G.; Smolin, Y. Y.; Soroush, M.; Lau, K. K. S., *Chem. Eng. Sci.* **2016,** *154*, 136. **DOI:** 10.1016/j.ces.2016.05.007.
41. Chen, N.; Reeja-Jayan, B.; Liu, A.; Lau, J.; Dunn, B.; Gleason, K. K., *Macromol Rapid Commun* **2016,** *37* (5), 446. **DOI:** 10.1002/marc.201500649.
42. Smolin, Y. Y.; Nejati, S.; Bavarian, M.; Lee, D.; Lau, K. K. S.; Soroush, M., *J. Power Sources* **2015,** *274*, 156. **DOI:** 10.1016/j.jpowsour.2014.10.028.
43. Stuart, M. A.; Huck, W. T.; Genzer, J.; Muller, M.; Ober, C.; Stamm, M.; Sukhorukov, G. B.; Szleifer, I.; Tsukruk, V. V.; Urban,

M.; Winnik, F.; Zauscher, S.; Luzinov, I.; Minko, S., *Nat Mater* **2010,** *9* (2), 101.
DOI: 10.1038/nmat2614.

44. Alf, M. E.; Hatton, T. A.; Gleason, K. K., *Langmuir* **2011,** *27* (17), 10691.
DOI: 10.1021/la201935r.
45. Yang, R.; Asatekin, A.; Gleason, K. K., *Soft Matter* **2012,** *8* (1), 31.
DOI: 10.1039/C1sm06334k.
46. McInnes, S. J.; Szili, E. J.; Al-Bataineh, S. A.; Xu, J.; Alf, M. E.; Gleason, K. K.; Short, R. D.; Voelcker, N. H., *ACS Appl Mater Interfaces* **2012,** *4* (7), 3566.
DOI: 10.1021/am300621k.
47. Montero, L.; Gabriel, G.; Guimera, A.; Villa, R.; Gleason, K. K.; Borros, S., *Vacuum* **2012,** *86* (12), 2102.
DOI: 10.1016/j.vacuum.2012.06.002.
48. Bose, R. K.; Lau, K. K. S., *Thin Solid Films* **2011,** *519* (14), 4415.
DOI: 10.1016/j.tsf.2011.01.288.
49. Unger, K.; Resel, R.; Coclite, A. M., *Macromol. Chem. Phys.* **2016,** *217* (21), 2372.
DOI: 10.1002/macp.201600271.
50. Pena-Francesch, A.; Montero, L.; Borros, S., *Langmuir* **2014,** *30* (24), 7162.
DOI: 10.1021/la5003594.
51. Alf, M. E.; Hatton, T. A.; Gleason, K. K., *Polymer* **2011,** *52* (20), 4429.
DOI: 10.1016/j.polymer.2011.07.051.
52. Wang, X.; Ugur, A.; Goktas, H.; Chen, N.; Wang, M.; Lachman, N.; Kalfon-Cohen, E.; Fang, W.; Wardle, B. L.; Gleason, K. K., *ACS Sensors* **2016,** *1* (4), 374.
DOI: 10.1021/acssensors.5b00208.
53. Jeong, B.; Bae, Y. H.; Lee, D. S.; Kim, S. W., *Nature* **1997,** *388* (6645), 860.
54. Lau, K. K.; Gleason, K. K., *Macromol Biosci* **2007,** *7* (4), 429,
DOI: 10.1002/mabi.200700017.
55. McInnes, S. J.; Szili, E. J.; Al-Bataineh, S. A.; Vasani, R. B.; Xu, J.; Alf, M. E.; Gleason, K. K.; Short, R. D.; Voelcker, N. H., *Langmuir* **2016,** *32* (1), 301.
DOI: 10.1021/acs.langmuir.5b03794.
56. Christian, P.; Ehmann, H. M. A.; Werzer, O.; Coclite, A. M., *Soft Matter* **2016**.
DOI: 10.1039/C6SM01919F
57. Christian, P.; Ehmann, H. M.; Coclite, A. M.; Werzer, O., *ACS Appl Mater Interfaces* **2016,** *8* (33), 21177.
DOI: 10.1021/acsami.6b06015.
58. Babu, N. J.; Nangia, A., *Cryst. Growth & Des.* **2011,** *11* (7), 2662.
DOI: 10.1021/cg200492w.
59. Ozaydin-Ince, G.; Gleason, K. K.; Demirel, M. C., *Soft Matter* **2011,** *7* (2), 638.
DOI: 10.1039/c0sm00922a.
60. Armagan, E.; Ozaydin Ince, G., *Soft Matter* **2015,** *11* (41), 8069.
DOI: 10.1039/c5sm01074h.
61. Perrotta, A.; Kessels, W. M.; Creatore, M., *ACS Appl Mater Interfaces* **2016,** *8* (38), 25005.
DOI: 10.1021/acsami.6b08520.
62. Aresta, G.; Palmans, J.; van de Sanden, M. C. M.; Creatore, M., *Microporous Mesoporous Mater.* **2012,** *151*, 434.
DOI: 10.1016/j.micromeso.2011.09.028.
63. Coclite, A. M.; Gleason, K. K., *J. Appl. Phys.* **2012,** *111*.
DOI: 10.1063/1.3702428.
64. Spee, D.; van der Werf, K.; Rath, J.; Schropp, R., *Phys. Status Solidi RRL* **2012,** *6* (4), 151.
DOI: 10.1002/Pssr.201206035.
65. Spee, D. A.; Bakker, R.; van der Werf, C. H. M.; van Steenbergen, M. J.; Rath, J. K.; Schropp, R. E. I., *Thin Solid Films* **2011,** *519*, 4479.
DOI: 10.1016/J.Tsf.2011.01.297.
66. Spee, D. A.; van der Werf, C. H. M.; Rath, J. K.; Schropp, R. E. I., *J. Nanosci. Nanotechnol.* **2011,** *11*, 8202.
DOI: 10.1166/jnn.2011.5100.
67. Servi, A. T.; Guillen-Burrieza, E.; Warsinger, D. M.; Livernois, W.; Notarangelo, K.; Kharraz, J.; Lienhard V, J. H.; Arafat, H. A.; Gleason, K. K., *J. Membr. Sci.* **2017,** *523*, 470.
DOI: 10.1016/j.memsci.2016.10.008.
68. Kim, D.; Im, H.; Kwak, M. J.; Byun, E.; Im, S. G.; Choi, Y. K., *Sci Rep* **2016,** *6*, 29993.
DOI: 10.1038/srep29993.
69. Sariipek, F.; Akin, I.; Arslan, G.; Karaman, M., *Vacuum* **2016,** *128*, 17.
DOI: 10.1016/j.vacuum.2016.03.003.
70. Matin, A.; Shafi, H.; Wang, M.; Khan, Z.; Gleason, K.; Rahman, F., *Desalination* **2016,** *379*, 108.
DOI: 10.1016/j.desal.2015.11.003.
71. Boscher, N. D.; Wang, M.; Gleason, K., *J. Mater. Chem. A* **2016**.
DOI: 10.1039/c6ta08003k.
72. Boscher, N. D.; Wang, M.; Perrotta, A.; Heinze, K.; Creatore, M.; Gleason, K. K., *Adv Mater* **2016,** *28* (34), 7479.
DOI: 10.1002/adma.201601010.
73. Seidel, S.; Dianat, G.; Gupta, M., *Macromol. Mat. Eng.* **2016,** *301* (4), 371.
DOI: 10.1002/mame.201500340.
74. Tufani, A.; Ince, G. O., *J. Appl. Polym. Sci.* **2015,** *132* (34).
DOI: 10.1002/app.42453.
75. Dianat, G.; Seidel, S.; De Luna, M. M.; Gupta, M., *Macromol. Mat. Eng.* **2016,** *301* (9), 1037.
DOI: 10.1002/mame.201600124.
76. Choi, J.; Seong, H.; Pak, K.; Im, S. G., *J. Inf. Disp.* **2016,** *17*, 43.
DOI: 10.1080/15980316.2016.1171803.
77. Seong, H.; Choi, J.; Jang, B. C.; Kim, M.; Yoo, S.; Choi, S.-Y.; Im, S. G., *Adv. Electron. Mat.* **2016,** *2* (5), 1500385.
DOI: 10.1002/aelm.201500385.
78. Jang, B. C.; Seong, H.; Kim, S. K.; Kim, J. Y.; Koo, B. J.; Choi, J.; Yang, S. Y.; Im, S. G.; Choi, S. Y., *ACS Appl Mater Interfaces* **2016,** *8* (20), 12951.
DOI: 10.1021/acsami.6b01937.